Nanoscale Advances

ROYAL SOCIETY OF CHEMISTRY

PAPER

View Article Online
View Journal | View Issue

Cite this: *Nanoscale Adv.*, 2023, **5**, 4286

New application of a periodic mesoporous nanocrystal silicon–silica composite for hyperlipidemia

Wenbin Lu,* Hao Jin,* Jiandong Ding, Yahao Zhang and Yong Wu

The integration of the properties of silicon nano crystallinity with silica mesoporosity provides a wealth of new opportunities for emerging biomedicine. Cholesterol (CHO) and triglyceride (TG) levels have always been a challenge for cardiologists in the treatment of patients with chronic coronary artery disease (CAD). For patients with hyperlipidemia, statins and other lipid-lowering drugs are currently recommended. It should be noted, however, that significant side effects have been reported in the treatments, including liver damage, muscle pain, *etc.* We here found that our previously produced periodic mesoporous nanocrystalline silicon–silica, meso-ncSi/SiO_2 (PMS), a nanocomposite material, has the properties of lowering CHO and TG, and is associated with better safety and biocompatibility compared to existing lipid-lowering drugs. After being incubated with PMS for 2 hours, CHO and TG levels in blood were significantly lower than before. In addition, CHO and TG adsorbed on with PMS could also be extracted and released, contributing to the recovery and recycling of PMS.

Received 28th June 2023
Accepted 8th July 2023

DOI: 10.1039/d3na00467h

rsc.li/nanoscale-advances

Background

According to the epidemiology of hyperlipidemia in the USA from 2007 to 2016, 48.6% to 57.9% of youths had elevated levels of cholesterol (CHO), high-density lipoprotein CHO, or non-high-density lipoprotein CHO,[1] which would contribute to an increased rate of cardiovascular events by 20% and total mortality by 12% with the levels of CHO increased by 1 mmol L^{-1}.[2,3] Based on the administrative databases of 3 Italian Local Health Units, one retrospective longitudinal cohort analysis showed that patients with higher triglycerides (TG) would have a higher risk of all-cause mortality (HR: 1.49, 95% CI: 1.36–1.63, $P < 0.001$) and incident atherosclerotic cardiovascular disease events (HR: 1.61, 95% CI: 1.43–1.82, $P < 0.001$) in comparison.[4] Based on an analysis of hyperlipidemia and medical expenditure among adults in the United States, it was observed that cardiovascular disease (CVD) patients with hyperlipidemia had higher expenditure ($1105), contributing to a $15.47 billion annual national expenditure.[5]

In addition to healthy lifestyle interventions, many therapies, including statins, fibrates, niacin, ezetimibe, and bile acid sequestrants are recommended for patients for reducing the level of blood lipids. In addition to the benefits, there are also limitations, such as myalgias, rhabdomyolysis, new-onset diabetes mellitus, blood transaminase elevation, an influence on appetite, *etc.*[2,6]

Recently, there has been growing interest in adsorbing agents such as resin and smectite, which have been found to effectively adsorb lipids and reduce weight. These agents have shown promising results in lipid adsorption. However, it is important to note that both resin and smectite exhibit poor biocompatibility, which is a significant drawback.[7–9]

Nowadays, silicon has been found to improve lipemia and insulin resistance, which would prevent atherogenic processes.[10] Additionally, a silicon-enriched diet would decrease very low-density lipoprotein (VLDL) concentrations and VLDL oxidation compared to a diet without silicon.[11] Based on silicon, our previously produced periodic mesoporous nanocrystalline silicon–silica, meso-ncSi/SiO_2 (PMS) was a nanocomposite material.[12] A groundbreaking approach for efficient organic functionalization of PMS was achieved by co-condensation of $(R'O)_3SiH$ and $(R'O)_3Si–R$ type terminal trialkoxy organosilanes. In the case of co-condensing MTES and TES, the organic PMS reached a maximum of 78% in the incorporation of the methyl group ($CH_3–SiO_3$ unit), which greatly broke the previous limit of 25%. Organic functionalization of PMS was an imperative and effective measure to advance its preeminent properties and widespread application due to its structural superiority.

Due to its ordered mesoporous structure, large surface area, and ease of functionalization, PMS exhibits excellent adsorption properties, which makes it an excellent solid-phase extraction adsorbent.[13,14] Moreover, various studies have demonstrated the ability of PMS to adsorb a variety of substances, such as gaseous species, liquids and solids.[15–17] Additionally, it was shown that co-administration of PMS in rats fed with a high-fat diet significantly reduced weight gain as

Department of Cardiology, Zhongda Hospital, Southeast University, 87#, Dingjiaqiao Road, Nanjing 210009, China. E-mail: 230219025@seu.edu.cn; luwenbinseu@163.com

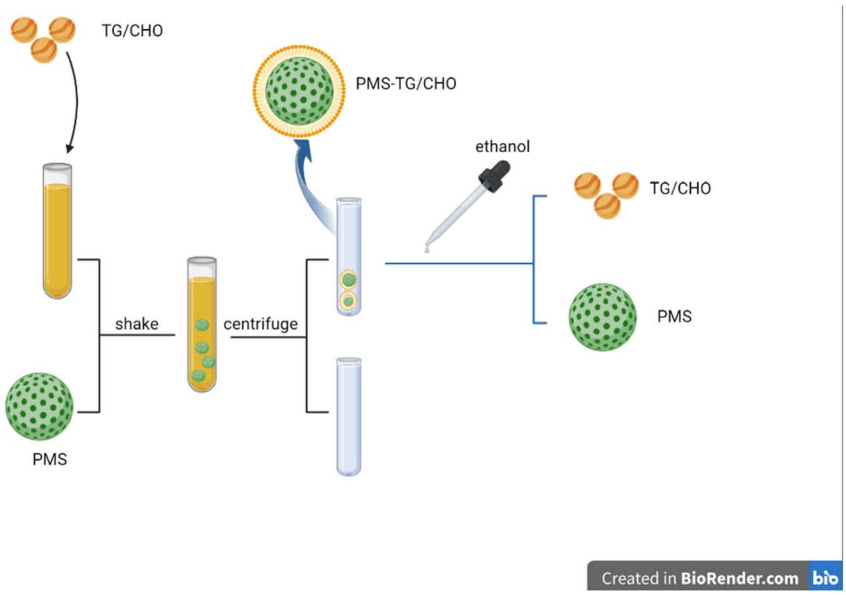

Fig. 1 Model diagram for CHO/TG adsorbed on PMS and separated from PMS. In brief, PMS was introduced into the CHO/TG solution to optimize the adsorption of CHO/TG onto PMS. Following centrifugation, the sediment was obtained, forming PMS-CHO/TG. Moreover, the addition of ethanol enabled the effective extraction and release of the adsorbed CHO/TG from PMS-CHO/TG.

compared to a negative control group, indicating that the PMS effectively adsorbed lipid substances within the gastrointestinal tract.[18] In recent years, PMS has demonstrated excellent biocompatibility within living organisms and has been widely used as a drug carrier through intravenous administration.[19–22] Nevertheless, it is unclear whether intravenous administration of PMS would further reduce blood lipid levels and atherosclerosis.

We therefore conducted this study to determine whether PMS is effective in reducing blood lipid levels. In our study, PMS was provided by the State Key Experiment in Biomedical Engineering at Southeast University. Overall, PMS was added into CHO/TG solutions to adsorb CHO/TG from solutions, and CHO/TG would also be separated from PMS (Fig. 1).

Experimental section

Various studies have demonstrated the ability of PMS to adsorb a variety of substances, such as gaseous species, liquids and solids.[15–17] Meaningfully, PMS could be successfully applied to adsorb the substances and the substances could be released. Especially for the adsorption of substances,[17] the adsorption amount of PMS could be determined by checking the concentration of substances in the supernatant. Similarly, the adsorption amount of PMS and the release characteristics of PMS for adsorbed substances could also be clarified. Similarly, our experiment was performed.

Material

Sigma-Aldrich (Germany) provided cetyltrimethylammonium chloride (CTAC), triethanolamine (TEA), tetraethyl orthosilicate (TEOS) and ethanol; standard CHO and TG were purchased from Nanjing Jiancheng Bioengineering Institute (China).

Synthesis of PMS

Cetyltrimethylammonium chloride (CTAC, 8 g) and triethanolamine (TEA, 0.068 g) were dissolved in turn in 20 mL of water at 95 °C under intensive stirring. After 1 h, 1.5 mL of tetraethyl orthosilicate (TEOS) was added dropwise and the resulting mixture was stirred for another hour. The products were collected by centrifugation and washed several times with ethanol to remove the residual reactants. Then, the collected products were extracted for 12 h with a mixture of ethanol and hydrochloric acid at 60 °C to remove the CTAC template. This process was carried out several times. Finally, residual surfactants and organics were completely removed by calcination at 450 °C and dispersed in water after ultrasonic and centrifugal cleaning three times.[23,24]

Characterization

Observation by means of transmission electron microscopy (TEM) (JEM-2100; JEOL, Tokyo, Japan): the particles were dispersed in ddH_2O and treated with ultrasound for 15 min to acquire the mixture for evaluation. The particles were dripped onto a 200-mesh copper TEM grid and dried afterwards. Finally, with the help of TEM, different images related to PMS were gathered. A nano particle potentiometer (Malvem, England) was used to measure the zeta potential and particle size of PMS before and after PMS adsorbed CHO and TG with the particles dissolved in PBS.

Preparation of a standard solution of CHO and TG

With the powder dissolved in ethanol, a standard solution of CHO (5.17 mmol L^{-1}) was synthesized. Similarly, a standard solution of TG (2.16 mmol) was also prepared with ethanol. Then, standard CHO and TG solutions were acquired, which were used for the following experiments independently.

The capacity of PMS for adsorbing CHO and TG in comparison to polystyrene resin

To adsorb the CHO from a solution with PMS, 10, 20, 40, 60, 80, and 100 μL of a standard CHO solution (5.17 mmol L^{-1}) were added into six 1.5 mL centrifuge tubes, in which 90, 80, 60, 40, 20, and 0 μL of water were then added respectively. Subsequently, 1 mg of PMS was added to each solution, which was dispersed and shaken at 4 °C for 2 h. Afterward, the solutions were centrifuged at 12 000 rpm at 4 °C for 10 min, the supernatant was then acquired to measure the concentration of CHO and the sediment was composed of PMS-CHO, which was washed twice with water. Finally, the capacity of PMS for adsorbing CHO was calculated based on the volume of CHO in the acquired supernatants and the previous solutions. Similarly, the supernatants of the TG solutions were acquired to test the concentration of TG and the sediment was composed of PMS-TG. The capacity of PMS for adsorbing TG was further calculated. In our study, we used polyethylene resin as the positive control group, considering its value in blood purification and lipid adsorption. In comparison, similar concentrations of CHO and TG solution were prepared, and 1 mg polystyrene resin was added into the centrifuge tubes respectively.

The capacity of PMS for adsorbing CHO and TG at different temperatures

According to our previous results, we evaluated the ability of PMS at different temperatures to adsorb CHO and TG from 60% of standard CHO solution (3.10 mmol L^{-1}) and TG solution (1.36 mmol L^{-1}), respectively.

In three 1.5 mL centrifuge tubes, 100 μL of CHO solution was added along with 1 mg of PMS, which was dispersed and shaken for 2 h at different temperatures, including 4 °C, 20 °C and 37 °C. Afterward, the solutions were centrifuged to obtain the supernatant, and the capacity of PMS to adsorb CHO at different temperatures could be determined.

Similarly, PMS's capacity to adsorb TG at different temperatures was assessed.

PMS for adsorbing CHO and TG in serum

To obtain serum, blood samples were centrifuged at 2000 rpm for 20 minutes and then heated to 80 °C for 1.5 minutes to remove lipases, which protect CHO and TG from hydrolysis. Furthermore, the serum was diluted in water to obtain the appropriate concentration, with the concentrations of CHO and TG adjusted to approximately 3.1 mmol L^{-1} and 1.2 mmol L^{-1}, respectively.

Safety assessment of PMS *in vivo*

L02 cells were inoculated into 96-well plates in an incubator set at 37 °C until more than 80% of the cells had been inoculated. Different concentrations of PMS (0–100 μg mL^{-1}) were added to the 96-well plate, with a total volume of 100 μL per well, and the culture continued for 24 hours. Afterwards, the proliferative ability of the cells was determined by CCK-8 reagent. During the experiment, the wells without cells served as a blank group. And the control group of cells was treated with 0 μg mL^{-1} of PMS.

$$\text{Cell viability} = \frac{\text{OD(experiment)} - \text{OD(blank)}}{\text{OD(control)} - \text{OD(blank)}}$$

Safety assessment of PMS in blood

As part of our study, blood was collected from 19 CAD 18–80 year-old patients, and safety parameters will be measured, including TBil (total bilirubin), DBil (direct bilirubin), IBil (indirect bilirubin), ALT (alanine aminotransferase), AST (aspartate aminotransferase), BUN (blood urea nitrogen) and Cr (creatinine). By mixing vitro blood with PMS and shaking it for 2 hours, safety parameters were obtained to evaluate PMS's safety. The Ethics Committee of Zhongda Hospital, Southeast University, China (approval number 2021ZDSYLL373-P01) approved all experiments. Informed consent was obtained from all subjects before samples were collected. The Ethics Committee of Zhongda Hospital approved and supervised all biosecurity, ethics and institutional safety procedures. Subjects were recruited in accordance with the Guidelines of the Declaration of Helsinki (Ethical Principles for Medical Research Involving Human Subjects, World Medical Association).

Comparison between PMS and statins for reducing CHO and TG

More importantly, PMS was added to the isolated blood of patients to judge its clinical role in reducing blood CHO and TG. 19 blood samples of patients visiting Zhongda Hospital affiliated to Southeast University were collected in our study. During our study, an automatic biochemical detector was used to test the blood lipids of the patients by collecting 5 mL of venous blood. A further 5 mL of venous blood was also obtained in order to assess the effect of PMS on lowering blood lipid. And 5 mL of venous blood was added to a 15 mL centrifuge tube and incubated with PMS. Then, an automatic biochemical detector was used to assess the level of blood lipids after shaking the mixture for two hours. Furthermore, the effectiveness of PMS in reducing blood cholesterol and triglycerides was compared. In our study, another 20 CAD patients taking a statin (atorvastatin 20 mg or rosuvastatin 10 mg) for at least 3 months were also enrolled in our study. And the lipid levels, including the levels of CHO and TG, were measured before and after statin treatment for 3 months. Furthermore, the lipid-lowering effect of a single use of PMS would be further compared with the lipid-lowering effect of statins used for 3 months.

Recovery and recycling of PMS

In order to determine the amount of CHO in PMS-CHO, the mixture was incubated with lipase for 30 minutes, then the CHO kit was used to measure the amount of CHO. Then, PMS-CHO was dispersed in 1000 μL of ethanol to separate PMS from CHO. Afterwards, when the mixture was centrifuged at 12 000 rpm at 4 °C for 10 minutes, the supernatant was obtained to determine the amount of CHO using the CHO kit,

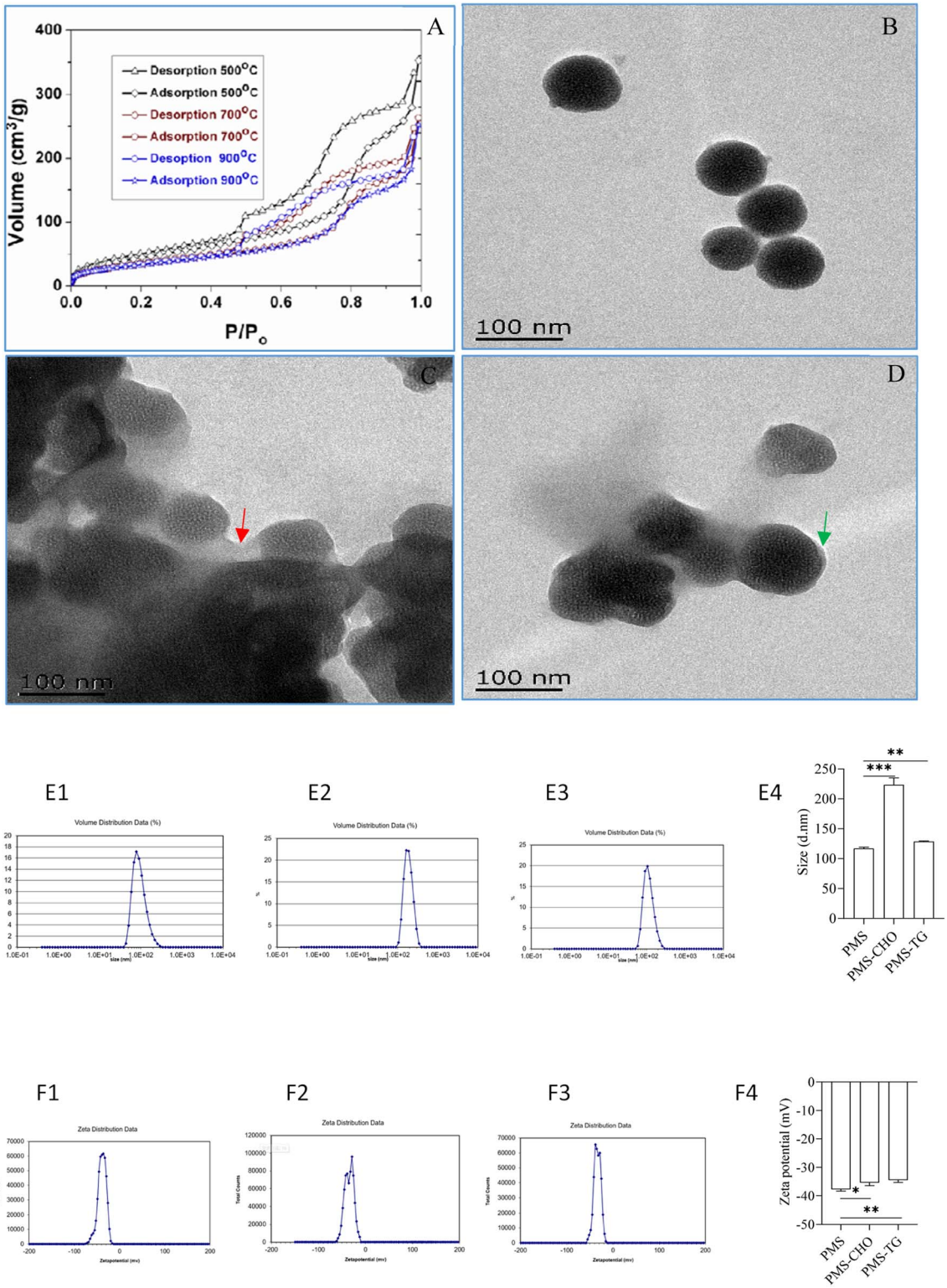

Fig. 2 Characterization of different PMS. (A) N_2 adsorption–desorption isotherms with thermal-treatment of PMS; (B) PMS without modifications; (C) PMS coated with CHO; (D) PMS coated with TG; (E) zeta potential of PMS; CHO: cholesterol; TG: triglyceride; (E1): size of PMS; (E2): size of PMS-CHO; (E3): size of PMS-TG; (E4) comparison of the size of different particles, including PMS, PMS-CHO and PMS-TG; (F1): zeta potential of PMS; (F2): zeta potential of PMS-CHO; (F3): zeta potential of PMS-TG; (F4) comparison of the zeta potential of different particles, including PMS, PMS-CHO and PMS-TG.

while the sediment was named PMS-CHO-1, which was used to determine the amount of remaining CHO on PMS using the lipase and CHO kits.

To determine the amount of TG in PMS-TG, PMS-TG was also incubated with lipase. In addition, PMS-TG was dispersed in ethanol to separate TG from PMS. After centrifugation, the supernatant and sediment (PMS-TG-1) were acquired to evaluate the amount of TG.

In order to evaluate whether PMS could be regenerated for repeated use, PMS-CHO and PMS-TG were washed with ethanol and water to obtain PMS. Such PMS was also obtained to determine PMS' capacity to adsorb CHO and TG, and the process was repeated several times.

Statistical analysis

GraphPad Prism 7.0 software (GraphPad Software Inc., La Jolla, CA, USA) was used for data analysis and statistical comparison between experimental groups. According to the distribution of the data, continuous data were expressed by mean ± standard deviation, median, or quartile; paired *t*-test was conducted in our analysis to make the comparison between the two groups. Results were considered statistically significant when the two-sided *P*-value was ≤0.05.

Results and discussion

Characterization

As described in our previous work, with photoluminescent silicon nanocrystallites embedded within a silica matrix throughout the mesostructure, PMS was finally produced, and N_2 adsorption–desorption isotherms with thermal treatment of PMS are shown in Fig. 2A.[25] TEM images revealed that the particles and pores were homogeneous when not adsorbing CHO or TG (Fig. 2B). In comparison, after incubation with CHO or TG, PMS was observed to be surrounded by CHO (indicated by red arrows; Fig. 2C) or TG (indicated by green arrows; Fig. 2D), which contributed to the poor dispersion of particles. The size characterization of PMS before and after adsorption revealed that the PMS particles adsorbing CHO (Fig. 2E2) and TG (Fig. 2E3) exhibited a significant increase in particle size compared to PMS (Fig. 2E1) without lipid adsorption. This difference was statistically significant (Fig. 2E4), indicating the successful adsorption of CHO and TG by PMS. With respect to potential changes of PMS before and after lipid adsorption, it was indicated that PMS (Fig. 2F1) without lipid adsorption exhibited a higher negative potential. In comparison, the surface negative potential of PMS after adsorbing CHO (Fig. 2F2) and TG (Fig. 2F3) decreased. And the difference was statistically significant (Fig. 2F4).

The capacity of PMS for adsorbing CHO and TG in comparison to polystyrene resin

In order to determine the ability of PMS to adsorb lipids, different concentrations of CHO have been used. As shown in Fig. 3A, PMS was mixed with different concentrations of CHO. Compared with CHO solutions with higher or lower concentrations, PMS showed better performance in the adsorption of lipids from a standard cholesterol solution with 60% concentration (3.1 mmol L^{-1}). According to Fig. 3B, PMS adsorbed TG most efficiently in a standard TG solution with a 60% concentration when TG was adsorbed at different concentrations (1.2 mmol L^{-1}). Similarly, a positive control group was treated with polyethylene resin. As shown in the figure, the resin exhibited strong adsorption capacity for CHO (Fig. 3C) and relatively weak adsorption capacity for TG (Fig. 3D).

The capacity of PMS for adsorbing CHO and TG at different temperatures

As shown in Fig. 4A, PMS showed a better performance for adsorbing CHO at lower temperature as compared to higher temperature. PMS also exhibited better performance at lower temperature when it came to adsorbing TG (Fig. 4B).

Safety assessment of PMS *in vivo*

The viability of L02 cells was determined using CCK-8 reagent after cells were incubated with different concentrations of PMS for 24 hours. As shown in the figure, PMS did not cause significant toxicity, even at higher concentrations (100 μg mL^{-1}) (Fig. 5).

Safety assessment of PMS in blood

We next analyzed the effect of PMS on blood biochemical indexes when lowering blood lipid; as shown in Table 1, there was no significant difference detected in terms of IBil (8.52 ± 3.42 *vs.* 8.12 ± 3.16, $p = 0.22$), ALT (22.68 ± 16.25 *vs.* 23.21 ± 16.39, $p = 0.18$) and BUN (6.82 ± 2.53 *vs.* 6.84 ± 2.52, $p = 0.43$). In comparison, PMS was associated with reduced TBil (12.31 ± 4.71 *vs.* 13.01 ± 4.71, $p < 0.001$), DBil (3.78 ± 2.24 *vs.* 4.88 ± 2.01, $p = 0.001$) and Cr (90.56 ± 46.86 *vs.* 93.06 ± 46.71, $p = 0.008$). These data indicated that PMS not only did not have negative effects on biochemical indicators such as IBil and ALT, but also had certain clearance effects on other biochemical metabolites such as DBil and Cr.

PMS was potent in lowering blood lipids in comparison with statin

The capacity of PMS for separating CHO and TG was first judged in the next study. With blood centrifuged at 2000 rpm (20 min), the serum was acquired and diluted with water to achieve a standard serum, with the concentration of CHO and TG at 3.1 mmol L^{-1} and 1.2 mmol L^{-1} respectively. After mixing with PMS and shaking for 2 h, the solution became more transparent and clearer, indicating that more CHO and TG were separated from the serum with PMS (Fig. 6). 19 whole blood samples were collected from patients. After being treated with PMS, the *in vitro* blood was identified with significant decreased levels of CHO (3.64 ± 1.01 *vs.* 3.71 ± 1.02, $p < 0.001$) and TG (1.43 ± 0.80 *vs.* 1.47 ± 0.82, $p < 0.001$) when compared to the control without intervention (Table 2).

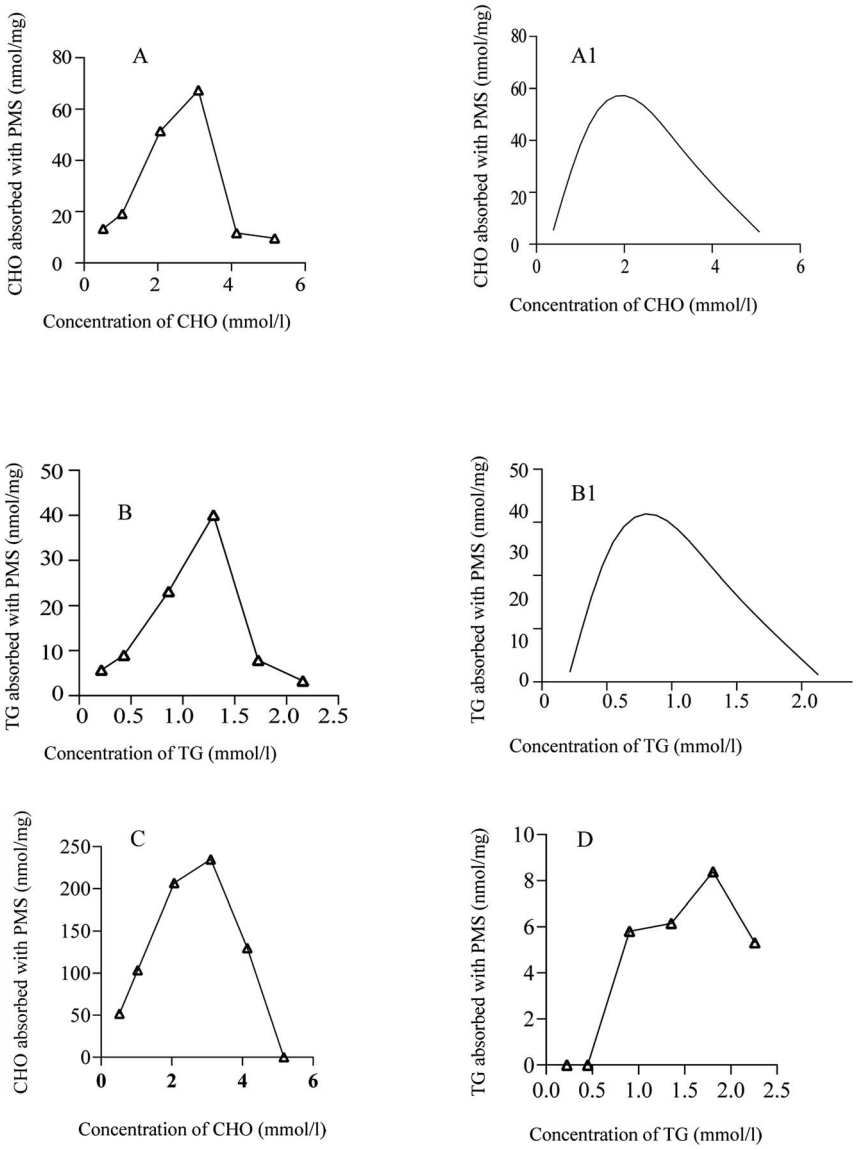

Fig. 3 The capacity of PMS for adsorbing CHO or TG at different concentrations. (A) The capacity of PMS for adsorbing CHO at different concentrations; (A1) fitted curve for PMS adsorbing CHO at different concentrations; (B) the capacity of PMS for adsorbing TG at different concentrations; (B1) fitted curve for PMS adsorbing TG at different concentrations; (C) the capacity of polystyrene resin for adsorbing CHO at different concentrations; (D) the capacity of polystyrene resin for adsorbing TG at different concentrations.

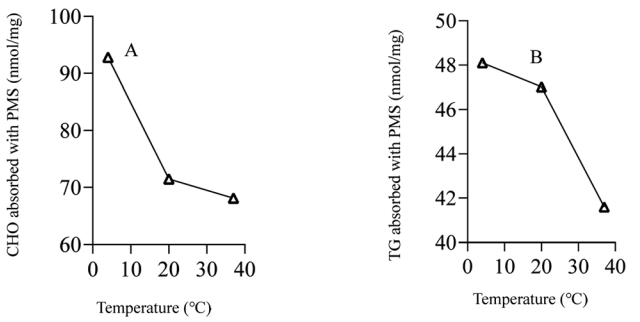

Fig. 4 The capacity of PMS for adsorbing CHO or TG at different temperatures. (A) The capacity of PMS for adsorbing CHO at different temperatures. (B) The capacity of PMS for adsorbing TG at different temperatures.

As a powerful lipid-lowering agent here, we further compared the difference between PMS and traditional statins in the degree of lipid-lowering ability for CAD patients. The efficacy of patients receiving statins for 3 months and the efficacy of one intervention with PMS were compared and are shown in Table 2. With respect to CHO, PMS was proved to be superior to statin (atorvastatin 20 mg or rosuvastatin 10 mg, 3 months) for reducing blood CHO ($p = 0.021$); with respect to TG, a single intervention with PMS achieved considerable results as against three months of statin treatment ($p = 0.685$) (Table 3).

Recovery and recycling of PMS

In practice, it was important to ensure that PMS could be regenerated for repeated use. In this study, PMS was mixed with

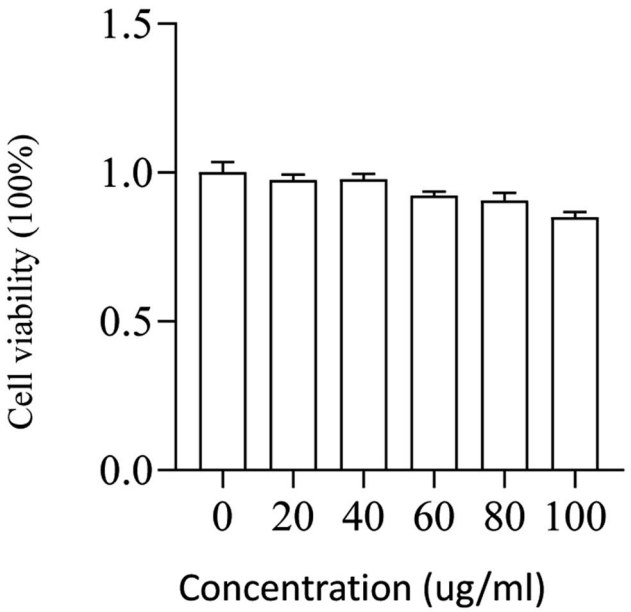

Fig. 5 Safety assessment of PMS in L02. The cell viability of L02 that was incubated with varying concentrations (0, 20, 40, 60, 80, 100 μg mL^{-1}) of the particles for 24 h.

a 60% standard concentration of CHO (3.1 mmol L^{-1}) or TG (1.2 mmol L^{-1}) to evaluate the regeneration of PMS.

With PMS-CHO mixed with lipase, 64.0 nmol of CHO was detected using a CHO kit. Afterward, PMS-CHO was treated with ethanol to release the adsorbed CHO. After centrifugation, the supernatant was acquired to determine the amount of CHO (61.6 nmol), and the sediment was composed of PMS-CHO-1, which was also mixed with lipase to evaluate the remaining amount of CHO on PMS (close to 0) (Fig. 7).

When treated with lipase, 38.8 nmol of TG was detected using a TG kit. With PMS-TG mixed with ethanol and centrifuged, 36.4 nmol of TG was detected in ethanol, while nearly 0 nmol of TG was detected in the remaining PMS-TG-1 (Fig. 8).

It has been shown in the figure that PMS can be used repeatedly, which was associated with a better capacity to adsorb CHO with different numbers of cycles, similar to TG (Fig. 9).

Adsorption mechanism

Zeta potential of the particles. Our study further investigated the mechanism of the role of PMS in lipid adsorption. As shown in Fig. 2F1–F4, PMS caused a decrease in the surface negative potential level after adsorbing CHO and TG.

This suggested that PMS adsorbed some positively charged substances, leading to a reduction in surface negative potential, which demonstrated the significant role of electrostatic attraction in the adsorption of PMS.

FT-IR and XPS. Furthermore, we conducted Fourier transform infrared (FTIR) and X-ray photoelectron spectroscopy (XPS) analyses on PMS before and after adsorption to further elucidate the adsorption mechanism. FTIR spectra were

Table 1 Safety assessment of PMS in blood[a]

	After the intervention	Before the intervention	*P* value
TBil, μmol L^{-1}	12.31 ± 4.71	13.01 ± 4.71	<0.001
DBil, μmol L^{-1}	3.78 ± 2.24	4.88 ± 2.01	0.001
IBil, μmol L^{-1}	8.52 ± 3.42	8.12 ± 3.16	0.22
ALT, U L^{-1}	22.68 ± 16.25	23.21 ± 16.39	0.18
BUN, mmol L^{-1}	6.82 ± 2.53	6.84 ± 2.52	0.43
Cr, μmol L^{-1}	90.56 ± 46.86	93.06 ± 46.71	0.008

[a] TBil: total bilirubin; DBil: direct bilirubin; IBil: indirect bilirubin; ALT: alanine aminotransferase; AST: aspartate aminotransferase; BUN: blood urea nitrogen; Cr: creatinine.

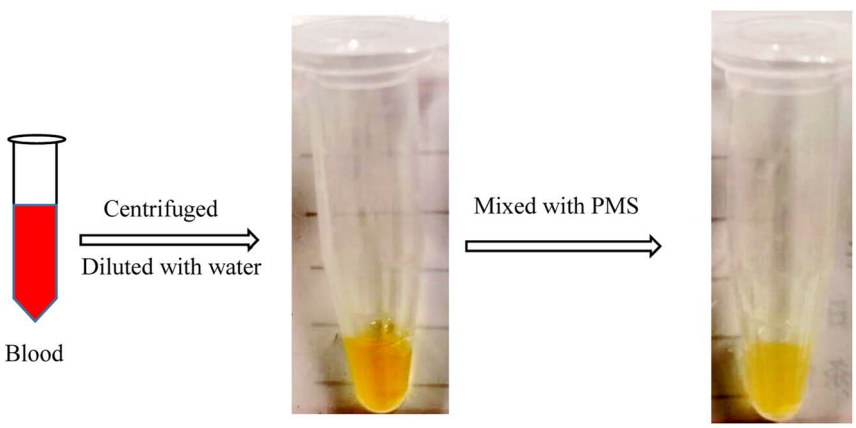

Fig. 6 PMS for adsorbing CHO and TG in serum. In brief, peripheral blood plasma was obtained from patients with atherosclerosis through centrifugation, and PMS was introduced for the adsorption of CHO/TG from the plasma, resulting in a visible lightening of the plasma color.

Table 2 PMS for reducing CHO and TG in patients' blood

	After the intervention	Before the intervention	*P* value
CHO, mmol L^{-1}	3.64 ± 1.01	3.71 ± 1.02	$P < 0.001$
TG, mmol L^{-1}	1.43 ± 0.80	1.47 ± 0.82	$P < 0.001$

Table 3 Comparison between PMS and statin for reducing blood CHO and TG

	Mesoporous silicas	Statin	*P* value
Reduced TG, mmol L^{-1}	0.03 (0.02, 0.04)	0.05 (−0.12, 0.36)	0.685
Reduced CHO, mmol L^{-1}	0.065 (0.035, 0.125)	0.33 (0.07, 1.55)	0.021

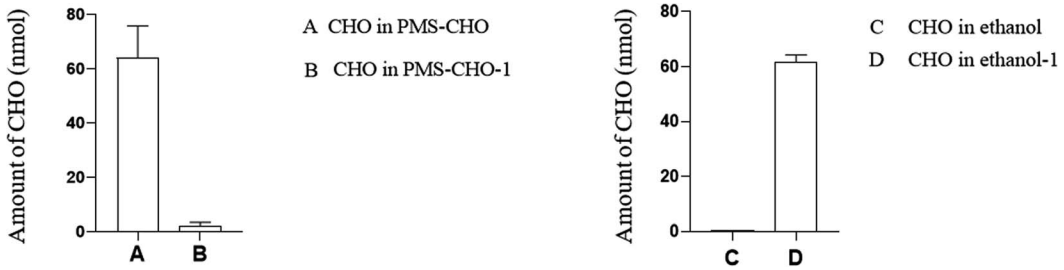

Fig. 7 Estimation and extraction of CHO on PMS. (A) The amount of CHO in PMS-CHO; (B) the amount of CHO in ethanol; (C) the amount of CHO in ethanol before PMS-CHO mixed with ethanol; (D) the amount of CHO in ethanol after PMS-TG mixed with ethanol.

recorded on a Nicolet 5700 spectrometer. And XPS was performed on a ThermoFisher Nexsa (USA). The data were processed using Origin 8.0.

The results, as shown in Fig. 10, revealed specific spectral changes upon CHO (Fig. 10A) adsorption. The peaks corresponding to hydroxyl groups (3400–3500 cm^{-1}) shifted backward and exhibited a noticeable decrease in transmittance. Additionally, changes in peak positions and intensities around 1500–1700 cm^{-1} and 1000 cm^{-1} are attributed to the vibrational modes of N–H and C–O functional groups. Similar spectral changes were observed for TG (Fig. 10B) adsorption.

XPS further analyzed the chemical structure of PMS and evaluated potential interactions during the adsorption process. The adsorbents before and after adsorption were examined for the adsorption of individual elements: carbon (C), nitrogen (N), oxygen (O), and silicon (Si).

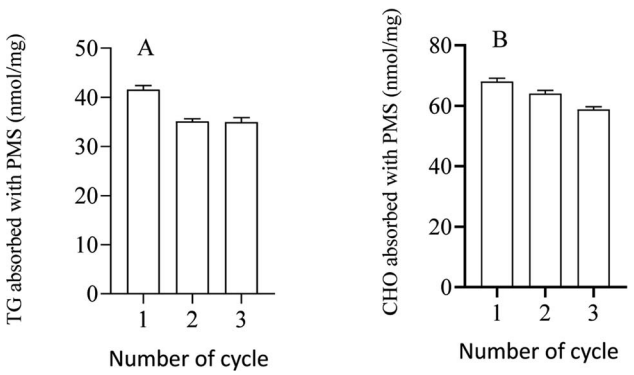

Fig. 9 The capacity of PMS for adsorbing CHO or TG with different numbers of cycles. (A) The capacity of PMS for adsorbing CHO with different numbers of cycles; (B) the capacity of PMS for adsorbing TG with different numbers of cycles.

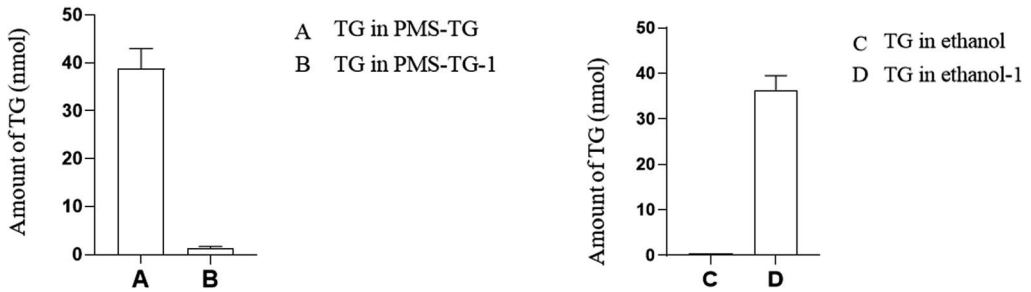

Fig. 8 Estimation and extraction of TG on PMS. (A) The amount of TG in PMS-TG; (B) the amount of TG in ethanol; (C) the amount of TG in ethanol before PMS-TG mixed with ethanol; (D) the amount of TG in ethanol after PMS-TG mixed with ethanol.

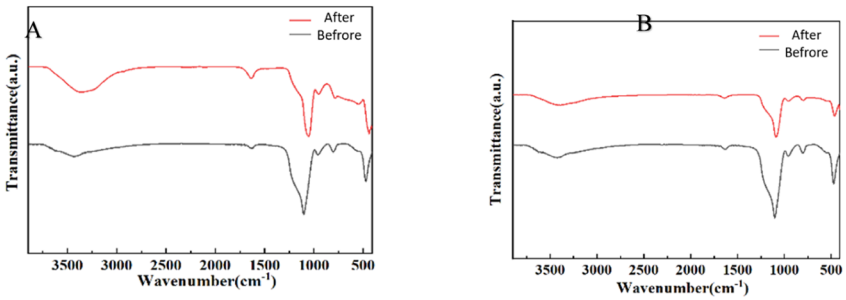

Fig. 10 FT-IR spectra of PMS before and after adsorbing CHO (A) and TG (B). Following the completion of CHO/TG adsorption by PMS, specimens were obtained both before (PMS) and after adsorption (PMS-CHO/TG). Spectral analysis was conducted on each specimen, and the spectral information regarding the changes in functional groups before (black line) and after adsorption (red line) was processed using Origin software.

Regarding CHO adsorption, the results, as shown in Fig. 11, revealed the following spectral changes: C 1s spectrum (Fig. 11A): three peaks at 284.82 eV, 286.45 eV, and 288.43 eV corresponded to C–C, C–N, and C–O, respectively. The binding energies of C–N and C–O decreased significantly in the adsorption process, while other bonds showed no significant changes. N 1s spectrum (Fig. 11B): two independent peaks representing N–H and C–N groups were observed at 399.64 eV and 402.43 eV, respectively, on PMS after lipid adsorption. The changes in C–N and N–H were evident compared to the pre-adsorption state. O 1s spectrum (Fig. 11C): the main peaks at 531.13 eV and 532.61 eV corresponded to O–H and C–O, respectively. During lipid adsorption, the main changes occurred in the O–H bonding. Si spectrum (Fig. 11D): the changes before and after adsorption were not significant.

In terms of XPS spectra, regarding CHO adsorption, the significant changes in binding energy and intensity of C–N, C–O, N–H and O–H suggested that amino groups were one of the primary functional groups responsible for lipid adsorption.

Similarly, for TG adsorption, the results, as shown in Fig. 12, indicated the following: C 1s spectrum (Fig. 12A): slight decreases in the binding of C–N were observed. N 1s spectrum (Fig. 12B): no significant changes were observed before and after adsorption with respect to decreasing the binding. O 1s spectrum (Fig. 12C): the main changes occurred in the O–H bonding during lipid adsorption. Si spectrum (Fig. 12D): the changes before and after adsorption were not significant.

These findings suggested that C–N, N–H, and O–H functional groups were primarily responsible for the adsorption of lipids.

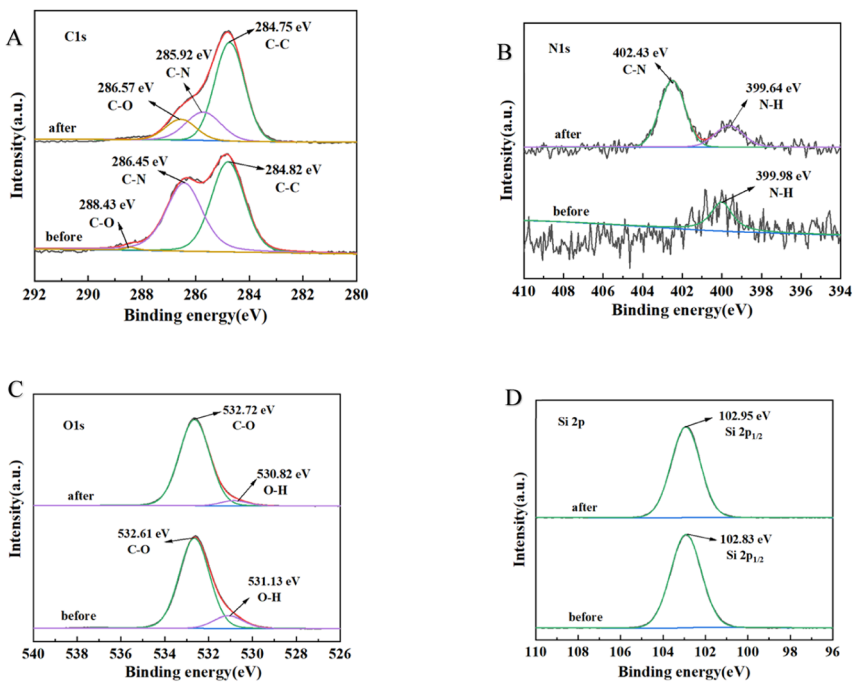

Fig. 11 C 1s (A), N 1s (B), O 1s (C) and Si 2p (D) XPS spectra of PMS before and after adsorbing CHO. Following the completion of CHO adsorption by PMS, specimens were obtained both before (PMS) and after adsorption (PMS-CHO). XPS spectra analysis was conducted on each specimen, and the spectral information regarding the changes was processed using Origin software, including C, N, O and Si.

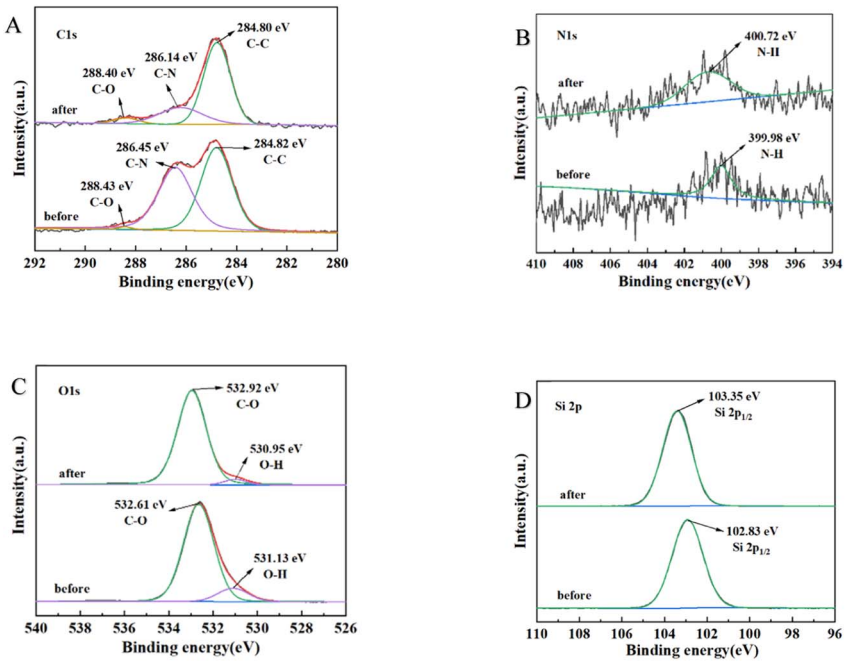

Fig. 12 C 1s (A), N 1s (B), O 1s (C) and Si 2p (D) XPS spectra of PMS before and after adsorbing TG. Following the completion of TG adsorption by PMS, specimens were obtained both before (PMS) and after adsorption (PMS-TG). XPS spectra analysis was conducted on each specimen, and the spectral information regarding the changes was processed using Origin software, including C, N, O and Si.

Discussion

In our study, PMS was associated with a greater capacity to adsorb CHO and TG, which could be released from PMS, contributing to its repeated use, which might be applied as a crucial component of an extracorporeal blood lipid purifier or treated as a lipid-lowering drug in the future.

First introduced by Mobil corporation scientists in 1992, associated with a tailored mesoporous structure, huge surface area, large pore volume, selective surface functionality, and morphology control, mesoporous silicon is more popular for biomedical application and has been applied to deliver drugs in the medical field, which has achieved great success.[26]

Similar to our findings, in obese mice treated with a high-fat diet, animals fed mesoporous silicas had significantly reduced body weight (6%) and body fat composition (12%) as compared with animals in the control group, demonstrating that mesoporous silicas reduce lipid absorption in the gastrointestinal tract.[27] However, Natalia *et al.* found that mesoporous silicas did not reduce blood lipid levels in a significant manner, which was different from our findings. In comparison, PMS was mixed with peripheral blood to reduce blood lipid levels in our study, while mesoporous silicas were added into the gastrointestinal tract and evaluated its influence on blood lipid levels in the study performed by Natalia *et al.*, which might partly explain this difference. In addition, another study was also performed to evaluate the effects of mesoporous silicas supplemented in food on metabolic parameters, which also conveyed a similar message that mesoporous silicas can successfully reduce adipose tissue formation from 9.4 to 6.5 g and leptin levels from 32.8 to 16.9 ng mL^{-1} respectively due to a 33% reduction in food efficiency.[28]

There are several factors that may contribute to the potential effect of PMS-based adsorbents on reducing blood lipid levels and improving atherosclerosis. Firstly, PMS contributed to the reduction of lipid levels in the blood by exerting various forces to adsorb blood lipids. Secondly, PMS–blood lipid complexes can interfere with the normal interaction between blood lipids and lipase, thereby disrupting the functionality of lipase. The combined effect of these two factors led to the reduction of blood lipid levels and improvement of atherosclerosis.

In terms of raw materials of PMS, silicon was reported to affect the metabolism of blood lipids. Silicon is a crucial component of the human body, measured in many tissues, such as the aorta, the tracheae, bones, skin, *etc.* A number of biological effects and disorders have been linked to silicon, including bone mineralization, collagen synthesis, aging of the skin, atherosclerosis, Alzheimer's disease, as well as many others.[29] As an explanation for silicon's role in reducing blood lipid levels, silicon is thought to form molecular crosslinks and contribute to the formation of ester bonds, which may contribute to reduced digestibility and bioavailability.[11]

Additionally, as demonstrated in this study, most CHO and TG on PMS could also be released when mixed with ethanol, demonstrating that CHO and TG were adsorbed or extracted from blood without any chemical reaction. Similarly, a previous study performed in 2018 found that mesoporous silicas could be used in solid-phase extraction for adsorbing phospholipids in human milk, which was associated with a higher adsorption capacity (544 μg of PC mg^{-1} of sorbent) and reusability (up to 15 reuses).[30]

Current research suggested that the specific adsorption mechanisms and forces of PMS on lipids are as follows: (1) PMS

contained Si–OH and Si–OSi bonds, which can interact with polar molecules through dipole–dipole interactions and hydrogen bonding, while the interaction with nonpolar molecules on the silica surface was weak.[31] Similar studies also acknowledged the importance of N–H and O–H in PMS adsorption.[32] Cholesterol molecules, being weakly polar, can enhance their interaction with PMS, making PMS more prone to adsorb cholesterol. This was consistent with our research findings, which demonstrated that PMS exhibited high adsorption capacity for weakly polar molecules such as CHO. Our FT-IR and XPS further supported this possibility. (2) The role of surface charge: although CHO and TG themselves were uncharged, they may acquire positive or negative charges upon dissolution, while PMS surfaces carry negative charges, which led to mutual attraction.[32] In our study, further zeta potential measurements confirmed the findings.

Regarding the cholesterol, a message was also conveyed that mesoporous silicas performed well in CHO separation, which was associated with 10–20, 40–60, and 50–65% of removal efficiencies for powder, crystal, and emulsion forms respectively.[33] More importantly, concerning the safety of PMS in clinical trials, no severe adverse events occurred in participants intaking mesoporous silicas (≥9 g per day) according to one single blinded safety study consisting of 20 males, which demonstrated the safety and tolerance of mesoporous silicas in humans.[34]

Limitation

A study we conducted showed that PMS was associated with enhanced CHO and TG adsorption, whereas most of these compounds were found in the form of lipoproteins in the blood. Consequently, PMS would affect the protein level in the blood when it was used to adsorb CHO and TG.

Moreover, we evaluated the effect of temperature on the capacity of PMS to adsorb CHO and TG, however, we did not assess the influence of pH, since acidic and alkaline environments would both contribute to the breakdown of CHO and TG.

In addition, no animal studies were conducted in our study to demonstrate the effects of PMS on lipid levels and the development of atherosclerosis. There is a need for further research to verify these findings.

Evaluation of the lipid-lowering effect of PMS in peripheral blood *in vivo* was constrained by the extended co-incubation time, which may give rise to thrombus formation and coagulation, impeding the interaction between PMS and lipids. As a result, the lipid-lowering effect of PMS in peripheral demonstrated *in vivo* was not prominently observed.

Conclusion

In this study, we have demonstrated a novel method for lowering blood lipids, which was safe, effective and recyclable. It was concluded that PMS was associated with reduced levels of blood lipids, which might be beneficial to hyperlipemia patients suffering from potential negative effects and prone to cardiovascular events. Additionally, most of the adsorbed blood lipids by PMS can also be released and extracted, contributing to the recovery and recycling of PMS.

Data availability

The authors declare that all the data in this manuscript are available upon request.

Author contributions

Jin and Lu conceived the experiments. Jin, Zhang and Wu conducted the experiments; Jin and Lu did data analysis and interpretation. All authors discussed the results.

Conflicts of interest

The authors declare no competing interests.

Acknowledgements

This work was supported by "The key research and development program of Jiangsu Province" (BE2021735) and the Youth Medical Talents Project of Jiangsu Province (No. QNRC2016814). We are grateful to the State Key Experiment in Biomedical Engineering at Southeast University for providing the PMS.

References

1 S. S. Virani, A. Alonso, E. J. Benjamin, M. S. Bittencourt, C. W. Callaway, A. P. Carson, A. M. Chamberlain, A. R. Chang, S. Cheng, F. N. Delling, L. Djousse, M. S. V. Elkind, J. F. Ferguson, M. Fornage, S. S. Khan, B. M. Kissela, K. L. Knutson, T. W. Kwan, D. T. Lackland, T. T. Lewis, J. H. Lichtman, C. T. Longenecker, M. S. Loop, P. L. Lutsey, S. S. Martin, K. Matsushita, A. E. Moran, M. E. Mussolino, A. M. Perak, W. D. Rosamond, G. A. Roth, U. K. A. Sampson, G. M. Satou, E. B. Schroeder, S. H. Shah, C. M. Shay, N. L. Spartano, A. Stokes, D. L. Tirschwell, L. B. VanWagner and C. W. Tsao, *Circulation*, 2020, **141**(9), e139–e596.

2 S. Fischer, U. Schatz and U. Julius, *Atheroscler. Suppl.*, 2015, **18**, 194–198.

3 Ž. Reiner, *Nat. Rev. Cardiol.*, 2017, **14**(7), 401–411.

4 M. Arca, C. Veronesi, L. D'Erasmo, C. Borghi, F. Colivicchi, G. M. De Ferrari, G. Desideri, R. Pontremoli, P. L. Temporelli, V. Perrone and L. Degli Esposti, *J. Am. Heart Assoc.*, 2020, **9**(19), e015801.

5 D. Zhang, G. Wang, J. Fang and C. Mercado, *Med. Care*, 2017, **55**(1), 4–11.

6 S. M. Grundy, N. J. Stone, A. L. Bailey, C. Beam, K. K. Birtcher, R. S. Blumenthal, L. T. Braun, S. de Ferranti, J. Faiella-Tommasino, D. E. Forman, R. Goldberg, P. A. Heidenreich, M. A. Hlatky, D. W. Jones, D. Lloyd-Jones, N. Lopez-Pajares, C. E. Ndumele, C. E. Orringer, C. A. Peralta, J. J. Saseen, S. C. Smith Jr, L. Sperling, S. S. Virani and J. Yeboah, *Circulation*, 2019, **139**(25), e1082–e1143.

7 T. J. Dening, P. Joyce, M. Kovalainen, H. Gustafsson and C. A. Prestidge, *Pharm. Res.*, 2018, **36**(1), 21.
8 A. Vuorio, J. Kuoppala, P. T. Kovanen, S. E. Humphries, S. Tonstad, A. Wiegman, E. Drogari and U. Ramaswami, *Cochrane Database Syst Rev*, 2019, **2019**(11), CD006401.
9 J. Pedro-Botet and X. Pintó, *Clin. Invest. Arterios.*, 2019, **31**(Suppl 2), 16–27.
10 J. Vidé, A. Virsolvy, C. Romain, J. Ramos, N. Jouy, S. Richard, J. P. Cristol, S. Gaillet and J. M. Rouanet, *Nutrition*, 2015, **31**(9), 1148–1154.
11 A. Garcimartín, J. A. Santos-López, S. Bastida, J. Benedí and F. J. Sánchez-Muniz, *J. Nutr.*, 2015, **145**(9), 2039–2045.
12 Z. Xie, E. J. Henderson, Ö. Dag, W. Wang, J. E. Lofgreen, C. Kübel, T. Scherer, P. M. Brodersen, Z. Z. Gu and G. A. Ozin, *J. Am. Chem. Soc.*, 2011, **133**(13), 5094–5102.
13 R. Schmid, N. Neffgen and M. Lindén, *J. Colloid Interface Sci.*, 2023, **640**, 961–974.
14 D. Wang, X. Chen, J. Feng and M. Sun, *J. Chromatogr. A*, 2022, **1675**, 463157.
15 M. Kang, J. T. Lee and J. Y. Bae, *Int. J. Mol. Med. Adv. Sci.*, 2023, **24**(4), 4208.
16 Z. Xiao, H. Bao, S. Jia, Y. Bao, Y. Niu and X. Kou, *Molecules*, 2021, **26**(9), 2744.
17 J. Tu, A. L. Boyle, H. Friedrich, P. H. Bomans, J. Bussmann, N. A. Sommerdijk, W. Jiskoot and A. Kros, *ACS Appl. Mater. Interfaces*, 2016, **8**(47), 32211–32219.
18 P. Joyce, T. J. Dening, T. R. Meola, A. Wignall, H. Ulmefors, M. Kovalainen and C. A. Prestidge, *ACS Appl. Bio Mater.*, 2020, **3**(11), 7779–7788.
19 S. S. Hate, S. M. Reutzel-Edens and L. S. Taylor, *Pharm. Res.*, 2020, **37**(8), 163.
20 F. Xie, Z. Xie, P. Liu, Y. Yuan, J. Li, S. Chen, F. Guo, J. Chen and Z. J. M. Gu, *Microporous Mesoporous Mater.*, 2018, S1387181118301197.
21 K. Trzeciak, A. Chotera-Ouda, S. Bak II and M. Potrzebowski, *J. Pharm.*, 2021, **13**(7), 950.
22 M. Lindén, *Enzymes*, 2018, **43**, 155–180.
23 Z. Xie, L. Bai, S. Huang, C. Zhu, Y. Zhao and Z. Z. Gu, *J. Am. Chem. Soc.*, 2014, **136**(4), 1178–1181.
24 L. Pan, Q. He, J. Liu, Y. Chen, M. Ma, L. Zhang and J. Shi, *J. Am. Chem. Soc.*, 2012, **134**(13), 5722–5725.
25 Z. Xie, E. J. Henderson, Ö. Dag, W. Wang, J. E. Lofgreen, C. Kübel, T. Scherer, P. M. Brodersen, Z.-Z. Gu and G. A. Ozin, *J. Am. Chem. Soc.*, 2011, **133**(13), 5094–5102.
26 Y. Zhou, G. Quan, Q. Wu, X. Zhang, B. Niu, B. Wu, Y. Huang, X. Pan and C. Wu, *Acta Pharm. Sin. B*, 2018, **8**(2), 165–177.
27 N. Kupferschmidt, R. I. Csikasz, L. Ballell, T. Bengtsson and A. E. Garcia-Bennett, *Nanomedicine*, 2014, **9**(9), 1353–1362.
28 M. Rinde, N. Kupferschmidt, M. N. Iqbal, G. Robert-Nicoud, E. V. Johnston, M. Lindgren and T. Bengtsson, *Nanomedicine*, 2020, **15**(2), 131–144.
29 L. M. Jurkić, I. Cepanec, S. K. Pavelić and K. Pavelić, *Nutr. Metab.*, 2013, **10**(1), 2.
30 H. Martínez Pérez-Cejuela, I. Ten-Doménech, J. El Haskouri, P. Amorós, E. F. Simó-Alfonso and J. M. Herrero-Martínez, *Anal. Bioanal. Chem.*, 2018, **410**(20), 4847–4854.
31 P. Samaddar, J. Hu, N. Barua, Y. Wang, T. A. Lee, M. Prodanović, Z. Heidari and T. Hutter, *ACS Omega*, 2022, **7**(47), 43130–43138.
32 T. Hua, D. Li, X. Li, J. Lin, J. Niu, J. Cheng, X. Zhou and Y. Hu, *Environ. Res.*, 2022, **215**(Pt 3), 114433.
33 A. Sinha, S. Basiruddin, A. Chakraborty and N. R. Jana, *ACS Appl. Mater. Interfaces*, 2015, **7**(2), 1340–1347.
34 E. Hagman, A. Elimam, N. Kupferschmidt, K. Ekbom, S. Rössner, M. N. Iqbal, E. Johnston, M. Lindgren, T. Bengtsson and P. Danielsson, *PLoS One*, 2020, **15**(10), e0240030.